Role of localized surface plasmons in surface-enhanced Raman scattering of shape-controlled metallic particles in regular arrays

J. Grand, M. Lamy de la Chapelle,* J.-L. Bijeon, P.-M. Adam, A. Vial, and P. Royer
LNIO, Université de Technologie de Troyes, 12 Rue Marie Curie, Boîte Postale 2060, 10010 Troyes Cedex, France
(Received 14 September 2004; revised manuscript received 2 February 2005; published 13 July 2005)

We studied the influence of localized surface plasmon resonance (LSPR) sustained by arrays of metallic nanoparticles on the efficiency of surface-enhanced Raman scattering (SERS). We found that the Raman enhancement that originates from the excitation of LSPR does depend on the particle shape. Two different shapes were investigated: cylindrical particles, for which the maximum of Raman enhancement occurred for a LSPR located around 650 nm, and ellipsoidal particles, which exhibit the strongest SERS signal at 700 nm. These results are compared to an analytical model in the quasistatic approximation. This model, though being quite simple, can give an explanation of the observed differences in terms of the lightning rod effect.

DOI: 10.1103/PhysRevB.72.033407 PACS number(s): 78.30.−j, 78.67.Bf, 78.20.Bh

I. INTRODUCTION

Surface-enhanced Raman scattering (SERS) has proven to be a powerful technique to observe very low concentrations of chemical species and even individual molecules.[1,2] To achieve SERS of single molecules, Kneipp *et al.*[2] took advantage of metallic colloidal solution to reach enhancement factors close to 10^{14}, whereas Nie *et al.*[1] used isolated metallic nanoparticles combined with resonant Raman spectroscopy. This huge enhancement arises mainly from an electromagnetic mechanism and also, to a lesser extent, from a chemical effect.[3] The latter mechanism is related to the charge transfer between the surface and the molecules and/or to the formation of chemical bonds between them resulting in a shift of the electronic energy levels. Its contribution to the SERS signal was estimated to be at most 10^2 on an overall average enhancement factor of at least 10^6.[3] In this paper, we do not focus our study on this effect but on the electromagnetic one, which involves the excitation of surface plasmons. We use metallic nanoparticle arrays that sustain localized surface plasmons (LSP) able to create, when excited resonantly, a huge electromagnetic field confined around the particles.[4] By varying the array parameters (particle size and shape, grating constant), the LSP resonance (LSPR) can be tuned over the whole visible range.[5,6] To understand the contribution of LSP to the enhancement of the Raman signal, we apply a method proposed by Haynes *et al.*[7] called the plasmon-sampled surface-enhanced Raman excitation spectroscopy (PS-SERES). This method consists of illuminating different samples, exhibiting a specific LSPR, each with a defined particle shape and size, with the same laser line and then plotting the Raman signal against the LSPR position. In this paper, we present the influence of LSPR on the Raman enhancement produced by SERS active substrates composed of cylindrical and ellipsoidal gold nanoparticles. We have also compared these results with an analytical model based on the quasistatic approximation.[4]

II. EXPERIMENT

Nanostructures of a desired shape, size, and arrangement are designed through electron beam lithography (EBL). To achieve EBL we operate a 30 kV Hitachi S-3500N scanning electron microscope (SEM) equipped with a nanometer pattern generation system (NPGS, by J. C. Nabity). Details of our EBL procedure are given in Grand *et al.*[6] This technique provides homogenous arrays of gold particles, as can be seen in Fig. 1(b). Each array covers an area of $80\times80\ \mu m^2$, which allows us to have several different arrays on the same sample. SERS-active substrates are immersed in a 10^{-3} M solution of *trans*-1,2-*bis*(4-pyridyl)ethylene (BPE) during 1 h and dried with nitrogen. Extinction[8] and Raman spectra are recorded on a modified Jobin-Yvon micro-Raman spectrometer (Labram) on the same zone of the sample with the same $\times10$ objective (N.A.=0.25) [Fig. 1(b)]. Raman measurements are carried out with the 632.8 nm line of a He-Ne laser and the intensity of the signal is estimated by calculating the area of a Lorentzian fitted BPE band located at 1200 cm^{-1} (this mode has a significant ethylenic C=C stretch character; see Ref. 9 for details). After the optical characterization

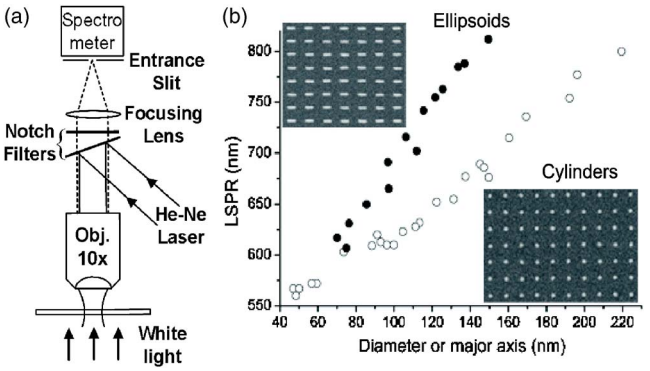

FIG. 1. (a) Experimental setup. Extinction spectroscopy: the sample is illuminated in transmission by a collimated light source and the notch filters are removed. Raman spectrum: classical backscattering configuration, using the 632.8 nm output of a He-Ne laser. (b) Variation of the LSPR wavelength with the diameter of cylinders (open circle) or the length of ellipsoids major axis (full circle). Inset: SEM images of typical arrays of ellipsoidal (minor axis: 50 nm, major axis: 120 nm, height: 50 nm) and cylindrical (diameter: 100 nm, height: 50 nm) particles achieved by EBL. The gap between two nanoparticles is kept constant at 200 nm.

and Raman measurements, the shape, lateral sizes, and height of the metallic nanoparticles are checked by combining the use of a SEM (Hitachi S-3500N) operating in low vacuum mode and an atomic force microscope (AFM) (Thermomicroscope CP-Research) operating in the tapping mode.

III. RESULTS

For ellipsoidal particles illuminated with linearly polarized light, the two LSP modes located in the substrate plane can be independently excited. These modes are spectrally separated, as is visible in Fig. 2(a), thereby giving different Raman intensity; in this case, when the laser polarization is set along the major axis, a strong Raman signal is recorded while only a very weak signal is acquired for a polarization direction along the minor axis [Fig. 2(b)]. Actually, the Raman intensity strictly follows the excitation of the LSP mode along the major axis, as shown in Fig. 2(c). This polarization dependence of the SERS signal and the LSPR intensity can be fitted with a square of the cosine function.[10] These synchronous variations indicate that the SERS signal arises from an electromagnetic mechanism and not from a chemical one. Throughout this article, to record the LSP and Raman spectra, the incident laser polarization is set parallel to the major axis of the ellipsoids.

By varying the cylinder diameter and the major axis length of the ellipsoidal particles, the LSPR is tuned over a wide range of wavelengths as shown in Fig. 1. Figure 3 presents the Raman signal plotted against the LSPR position. To avoid any artifactual measurements, the same experiments have been repeated with several samples. For each kind of particle, the Raman signal has been normalized to the most intense spectrum. Both cylindrical and ellipsoidal particles exhibit a maximum of Raman enhancement for a specific LSPR and yield no measurable signal far away from it. The position of this maximum differs from cylindrical to ellipsoidal particles, the highest enhancement being obtained for a LSPR around 650 and 700 nm, respectively. Moreover, both curves display a shoulder at approximately 700 nm for cylinders and 650 nm for ellipsoids. Whatever the differences between the two Raman intensity curves, one can observe that the Raman enhancement occurs within the same wavelength range (namely 600–750 nm). Such an observation suggests the existence of two components in the experimental curves: one at 650 nm and another at 700 nm.

In order to explain the link between LSPR position and Raman enhancement, Wokaun[4] proposed the following expression for the Raman enhancement factor, g, in the quasistatic approximation:

$$g = |f(\lambda_0) \cdot f(\lambda_R)|^2, \tag{1}$$

where

$$f(\lambda) = \frac{V}{2\pi l^3} \frac{\epsilon(\lambda) - 1}{1 - [1 - \epsilon(\lambda)]A_{\text{eff}}}, \tag{2}$$

where λ_0 and λ_R are, respectively, the incident laser and Raman wavelengths, V is the particle volume, l is the half-length of the particle axis parallel to the excitation polarization, $\epsilon(\lambda)$ is the material dielectric function, and A_{eff} is the effective depolarization factor described in Ref. 4,

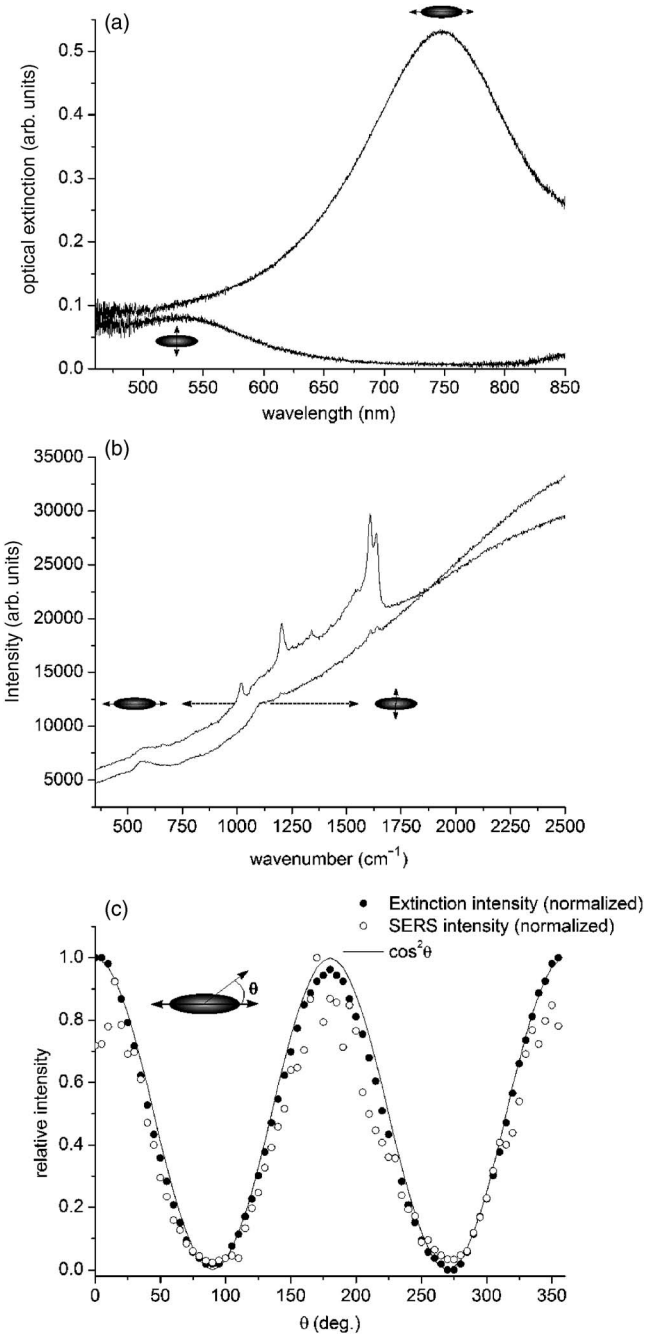

FIG. 2. (a) Extinction spectra of an ellipsoidal particle array (major axis: 120 nm, minor axis: 50 nm, height: 50 nm) for two polarization directions of the incident light, parallel and perpendicular to the major axis. (b) Raman spectra of the BPE recorded for two polarization directions of the incident laser, parallel and perpendicular to the major axis. (c) Raman (open circle) and LSPR (mode along the major axis located at 750 nm, full circle) intensity plotted against the polarization angle (0° is for a polarization parallel to the major axis); the solid line is the $\cos^2$ fit.

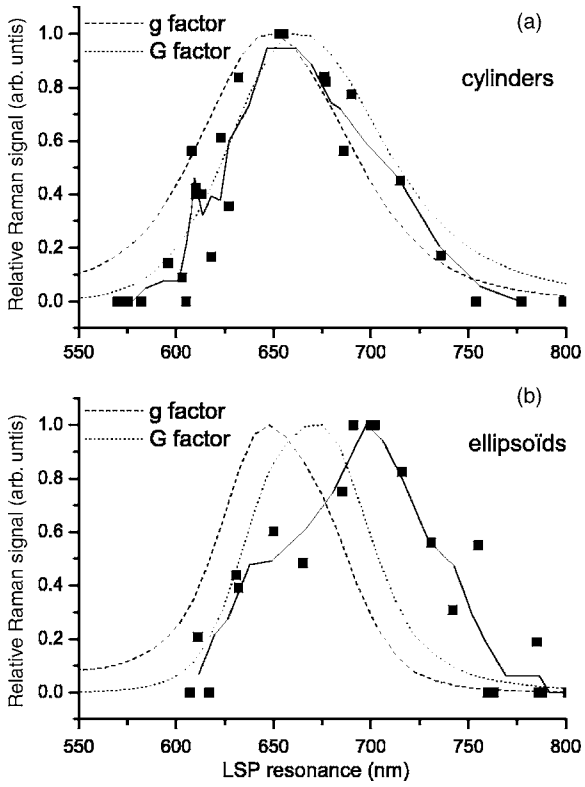

FIG. 3. Raman intensity of the 1200 cm^{-1} BPE line vs LSPR: (a) for cylinders, (b) for ellipsoids. Solid lines are the binned average values of the LSPR and the Raman intensity. The dashed and dotted lines are the calculated curves (dashed line: *g* factor, dotted line: *G* factor).

$$A_{\mathrm{eff}} = A - \frac{4\pi^2}{3\lambda^2} V^{2/3} - i\frac{4\pi^2 V}{3\lambda^3}, \tag{3}$$

where the latter factors take into account the shape of the particle (A is the pure geometrical consideration) and some first order corrections to the quasistatic model [$(4\pi^2/3\lambda^2)V^{2/3}$ is dynamic depolarization,[11] $i(4\pi^2 V/3\lambda^3)$ is radiation damping[4]].

According to formula (1), the enhancement factor consists in two different terms: $f(\lambda_0)$, which stems from the particle near-field enhancement at the incident wavelength, and $f(\lambda_R)$ arising from the reradiation of the molecule Raman near-field by the particle. According to this model, the best enhancement should be located between λ_0 and λ_R, as observed experimentally by Haynes *et al.*[7] It has also been suggested that it may occur for a LSPR close to the average of the excitation wavelength and the Raman wavelength.[12,13] Since we illuminate our samples at $\lambda_0 = 632.8$ nm and use the 1200 cm^{-1} band ($\lambda_R = 684.8$ nm) to calculate the Raman signal, the maximum of enhancement should be obtained for a LSPR between these two values. For other Raman bands, the experimental curves should be up- or downshifted when the Raman wavelengths increases or decreases, respectively.

Regarding experimental data for cylindrical particles, the evolution of the Raman signal with respect to the LSPR is in agreement with the rule given in Ref. 13 since the maximum of enhancement is experimentally found at approximately 650 nm. However, it is not suitable for ellipsoidal nanoparticles that yield a maximum of Raman signal around 700 nm. To determine the origin of the differences between cylinders and ellipsoids, the LSPR and the associated enhancement factor has been calculated for different kinds of nanostructures. Cylinders were approximated as oblate particles and ellipsoids as prolate (Fig. 3).[14] The calculations were carried out with nanostructures surrounded by air, the incident light being polarized along the longer axis of cylindrical (diameter) and ellipsoidal (major axis) particles.

For cylindrical particles, we obtain with the analytical model a symmetrical curve (Gaussian shape) exhibiting a maximum of enhancement around 640 nm. This maximum is close to the experimental one. However, we can notice a deviation of the theoretical curve from the experimental one for short wavelengths. To improve the model, it is possible to take into account an effect induced by the particle geometry: the tip effect, also known as lightning rod effect. The tip effect actually implies some accumulation of charges at the particle extremities, thus generating large enhancement, especially for nonsymmetrical structures such as ellipsoids. Hence the new expression of the electrical field enhancement derived by Wokaun,[4]

$$G = \gamma^4 \phi |f(\lambda_0) \cdot f(\lambda_R)|^2. \tag{4}$$

γ is a purely geometrical factor and ϕ is an "attenuation factor," introduced to offset the enhancement induced by the previous factor by averaging the electrical field over the whole particle surface (see Ref. 4 for more details). The results of the calculations are presented in Fig. 3. The dotted curves represent the Raman enhancement including the lightning rod effect correction. We can see that, for cylindrical particles, this curve is slightly redshifted (maximum close to 660 nm) compared to the case where no tip effect is considered ("*g* factor" curve that exhibits a maximum at 650 nm). Taking into account the lightning rod effect also reproduces the asymmetrical shape of the experimental curve. Thus, such a model provides a good approximation of the SERS experiments for cylindrical geometry.

For ellipsoidal particles, with or without the tip effect correction, the analytical model does not fit the experimental points. Nevertheless, the theoretical model can help us to explain the observations on ellipsoidal particles. If we do not take into account the tip effect, we obtain a curve with a maximum close to 650 nm and a shoulder at 675 nm. The tip effect being taken into consideration, the curve now exhibits a maximum at 675 nm and a shoulder around 650 nm. Thus, for ellipsoidal particles, two components to the Raman enhancement can be found on the theoretical curve. The first one at 650 nm corresponds to equivalent contributions of $f(\lambda_0)$ and $f(\lambda_R)$, whereas, for the second one located at 675 nm, there is a prominence of $f(\lambda_R)$. Their relative intensity will depend on the tip effect. Indeed, from the shape of the curve, we can assess that the tip effect favors the reradiation of Raman scattering by the nanoparticles and then strengthens the $f(\lambda_R)$ contribution. This observation can also give information on the cylindrical particle behavior. Indeed, as mentioned above, the calculations including the lightning rod

effect (G factor) for cylindrical particles exhibit an asymmetrical shape on the high wavelength side. This shape can be assigned to an increase of the relative intensity of the Raman signal reradiation process. On the contrary, for cylindrical particles, the theoretical curve without tip effect is symmetrical with no enhanced contribution of the reradiation process. In this way, in experimental cases, the two components observed at 650 and 700 nm on experimental curves are related to two contributions. The first one is the classical SERS enhancement factor (g) and is located at the average between λ_0 and λ_R, whereas the second one is favored by the tip effect at the Raman wavelength λ_R.

The nanoparticles with ellipsoidal shape are largely more influenced by the tip effect than the cylinders. In this case, the differences between cylinders and ellipsoids observed for the Raman enhancement can be assigned to the tip effect; the more this effect is enhanced, the more the reradiation process is favored.

IV. CONCLUSION

Our results support the fact that the optimization of SERS efficiency, relative to the LSPR, strongly depends on the shape of the metallic nanoparticles. Moreover, these experiments confirm that the maximum of Raman enhancement is obtained for a LSPR located between λ_0 and λ_R. However, the assumption that this enhancement should be maximum for a LSPR wavelength situated halfway between λ_0 and λ_R is not verified for all particle shapes. This rule is satisfied by particles with a cylindrical shape, but fails to explain the position of the maximum of enhancement for ellipsoids. Actually, in the enhancement process, both parts of the enhancement factor, $f(\lambda_0)$ and $f(\lambda_R)$, have their contributions modified by the shape of the nanostructures. The process of Raman reradiation seems to be all the more favored by the tip effect and then by elongated particles. For particles which have a large aspect ratio (length/diameter) such as ellipsoids, the nanoparticles better play the role of nanoantenna for the Raman radiation and, as a consequence, the best enhancement is observed for LSPR close to λ_R.

ACKNOWLEDGMENTS

The authors acknowledge the Conseil Régional de Champagne-Ardenne, the European Regional Development Fund, and the European Social Funds for financial support.

*Corresponding author. Electronic address: marc.lamy_de_la_chapelle@utt.fr

[1] S. Nie and S. R. Emory, Science **275**, 1102 (1997).
[2] K. Kneipp, Y. Wang, H. Kneipp, L. T. Perelman, I. Itzkan, R. R. Dasari, and M. S. Feld, Phys. Rev. Lett. **78**, 1667 (1997).
[3] M. Moskovits, Rev. Mod. Phys. **57**, 783 (1985).
[4] A. W. Wokaun, *Solid State Physics*, edited by H. Ehrenreich, F. Seitz, and D. Turnbull (Academic, New York, 1984), Vol. 38, p. 223.
[5] T. R. Jensen, M. D. Malinsky, C. L. Haynes, and R. P. Van Duyne, J. Phys. Chem. B **104**, 10549 (2000).
[6] J. Grand, S. Kostcheev, J. L. Bijeon, M. L. de la Chapelle, P. M. Adam, A. Rumyantseva, G. Lrondel, and P. Royer, Synth. Met. **139**, 621 (2003).
[7] C. L. Haynes and R. P. Van Duyne, J. Phys. Chem. B **107**, 7426 (2003).
[8] P. Royer, J. L. Bijeon, J. P. Goudonnet, T. Inagaki, and E. T. Arakawa, Surf. Sci. **217**, 384 (1989).
[9] W. Yang, J. Hulteen, G.-C. Schatz, and R. P. Van Duyne, J. Chem. Phys. **104**, 4313 (1996).
[10] T. Itoh, K. Hashimoto, and Y. Ozaki, Appl. Phys. Lett. **83**, 2274 (2003).
[11] M. Meier and A. Wokaun, Opt. Lett. **8**, 581 (1983).
[12] N. Félidj, J. Aubard, G. Lévi, J. R. Krenn, M. Salerno, G. Schider, B. Lamprecht, A. Leitner, and F. R. Aussenegg, Phys. Rev. B **65**, 075419 (2002).
[13] N. Félidj, J. Aubard, G. Lévi, J. R. Krenn, A. Hohenau, G. Schider, A. Leitner, and F. R. Aussenegg, Appl. Phys. Lett. **82**, 3095 (2003).
[14] The parameters for oblate particles are the following: height =50 nm, diameter=50–300 nm. For prolates: height=50 nm, width=50 nm, and length=50–300 nm. For oblate, the height has to be lower than the experimental one otherwise the LSPR will not be in the experimental range (550–800 nm).